Transport and Fate of All-Time Released Plastics in the Global Ocean

Peipei Wu[1†], Ruochong Xu[1†], Xuantong Wang[1†], Amina T. Schartup[2], Arjen Luijendijk[3,4], Yanxu Zhang[1*]

[1]School of Atmospheric Sciences, Nanjing University, Nanjing, China.

[2]Scripps Institution of Oceanography, University of California at San Diego, La Jolla, CA, USA.

[3]Faculty of Civil Engineering and Geosciences, Delft University of Technology, Delft, Netherlands.

[4]Hydraulic Engineering, Deltares, Delft, Netherlands.

[*]Correspondence to: zhangyx@nju.edu.cn

[†]These authors contributed equally to this work.

Abstract

Mismanaged plastics accumulate in oceans and threaten marine life. About 40 million tonnes of plastics have reached the oceans, where their fate remains unclear. To track the sources, sinks, sizes, and age of all-time released plastics, we developed a new mechanistic model and synthesized decades of measurements. We find that Asian plastics are the largest contributor (76%) to marine plastics by mass but only affect the North Pacific and the Indian Ocean, whereas plastics from fishing and shipping activities contribute 24% by mass but cover 60% of the ocean surface. Using the model, we demonstrate that biologically productive nearshore (63%) or upper ocean (25%) ecosystems trap 88% of the marine plastic. This study provides a model framework to assess the potential effect of future mitigation strategies.

Introduction

Plastics are durable, versatile, and ubiquitous in modern life. While their production has increased from 1.7 million tonnes in 1950 to 300 million tonnes per year today, plastic waste management has not kept up, resulting in >1 million tonnes of plastics entering the oceans every year (Lebreton et al., 2017). Plastics are causing physical problems for wildlife, and the harmful chemical additives mixed into plastic polymers for improved performance (e.g. bisphenol A, lead) are leaching into the environment (Mato et al., 2001, Teuten et al., 2009, Gregory, 2009). After seven decades of production, they are found in coastal areas, subtropical gyres (Eriksen et al., 2014 , Cozar et al., 2014), and remote areas such as the polar regions and deep seafloors (Lusher et al., 2015a, Peeken et al., 2018, Lacerda et al., 2019, Fischer et al., 2015). Reducing marine plastic pollution is the leading target of the United Nations' Sustainable Development Goals for ocean pollution (https://www.un.org/sustainabledevelopment/).

Despite the large discharge, less than 1% of the accumulated discharge is estimated to float at the surface (Koelmans et al., 2017). Where the remaining 99% "missing plastics" are remains unclear but assumed to settle below the surface (Koelmans et al., 2017) and deep seafloor is a major sink (Kane et al., 2020 , Woodall et al., 2014). Numerical models have been developed to study the transport of global marine plastics (Lebreton et al., 2012 , Van Sebille et al., 2012 , Wichmann et al., 2019 , Mountford and Morales Maqueda, 2019), but most focused on the

surface ocean, considered only the drifting process of plastic particles, or not included the historical discharge since they began to be used. Here we develop a three-dimensional global ocean model and use it to track the sources, sinks, sizes, and age of all-time released plastics. We use marine plastic measurement data and develop a new mechanistic model that considers the plastic source scenarios with historical trends since the 1950s and the primary processes that plastics undergo in seawater: drifting, beaching, settling, biofouling/defouling, abrasion, and fragmentation (see Methods).

Results and Discussion

Transport and Fate. The model reveals large spatial variability for plastic distribution in the surface ocean (defined here as the top 0.5 m) and successfully replicates the development of "Garbage Patches" in the subtropical ocean gyres in both hemispheres (Fig. 1A, 1D). In these regions with anticyclonic wind stress, Ekman transport results in a convergence zone that concentrates buoyant plastics (Lebreton et al., 2012). We calculate that the vertical-integrated concentrations of plastics accumulating in these regions range between 0.078-2.1 kg km^{-2}, which are consistent with observations (Cozar et al., 2014 , Eriksen et al., 2014 , Reisser et al., 2013). Compared with the northern hemisphere, accumulation zones in the South Pacific Ocean and South Atlantic Ocean present lower modeled concentrations (0.078-0.63 kg km^{-2}) due to the lower riverine plastic discharge (Schmidt et al., 2017 , Lebreton et al., 2017). The model allows us to identify additional zones of plastic accumulation. Heavy discharge from East Asia results in 0.16-36 kg km^{-2} in the western subtropical Pacific Ocean (especially the coastal regions). Simulated concentrations near the discharge points along the coastlines of South Asia and Europe are also relatively high (up to 22 kg km^{-2}). High concentrations are modeled in the Atlantic sector of the Arctic Ocean (0.83 kg km^{-2}) due to intense fishing and ship traffic (Lusher et al., 2015b).

The model considers the transport and fate of common plastics: Polyethylene (PE), Polypropylene (PP), Polyvinyl chloride (PVC), and lumped others with smaller discharges and similar density to seawater. All types are found in ocean basins but show different spatial distribution patterns. PE and PP have an initial density lower than the seawater while PVC and the others are denser or similar to seawater. Thus PE and PP float in the ocean surface for even seventy years and are easily transported by surface ocean currents and winds. They travel far from source regions (river mouth or the open ocean where shipping/fishing activities occur) and accumulate in subtropical gyres (Fig. 1D). In contrast, PVC tends to sink near sources and does not converge in open ocean gyres (Fig. 1E).

We estimate that 9.9×10^4 tonnes (ranging from 7.9×10^4-1.7×10^5 tonnes) plastics are present in the global surface ocean, of which ~45% are microplastics (defined as diameter < 5 mm) and ~55% are macroplastics (defined as diameter > 5 mm) (Fig. 2, Fig. S10). This mass represents a small fraction (0.25%) of all the plastics that entered the oceans between 1950-2018. The model estimates that there are 2.0×10^{12} catchable plastic particles (i.e. > 0.33 mm that is the mesh size of the towing net often used for plastic measurements), weighting 9.5×10^4 tonnes afloat on sea surface. The modeled spatial distribution of plastic concentrations is generally consistent with previous measurements (Fig. 1A). The observed mass concentrations span more than five orders of magnitudes, while our model simulates a narrower range and the modeled number concentrations are also lower (Fig. S1). This inconsistency may come from the uncertainty of the size distribution of riverine discharge inventories and the model parameterizations (see Uncertainty Analysis).

The previous estimate for the plastic mass in the global surface ocean spans a wide range. Our estimate of total afloat mass is one order of magnitude higher than the result of Cózar et al. (7.0×10^3 - 3.5×10^4 tonnes), but they considered only the surface convergence zones (Cozar et al., 2014). In addition, we model the change of the density of plastic particles influenced by phytoplankton attachment/detachment (aka biofouling/defouling) (Kooi et al., 2017). The upward movement of plastics (e.g. the effect of upwelling and the re-rise due to reduction in density caused by defouling) in the three-dimension model also increases the mass of plastics in the surface ocean. Indeed, Eriksen et al. and Koelmans et al. brought the estimate higher (2.7×10^5 tonnes and 3.1×10^5 tonnes, respectively) by considering the vertical distribution of plastics in the seawater or modeling more processes like sedimentation and fragmentation (Eriksen et al., 2014, Koelmans et al., 2017), which is close to our high-end estimate. Other estimations that are higher than ours are due to the differences in parameterizing the plastic transport and transformation processes (Lebreton et al., 2019, Van Sebille et al., 2015).

The model estimates that most of the total plastics entering the oceans are held by beaches (42%) and benthic sediment (31%) with the remaining 27% in the water column (Fig. 2). Among the plastics in the water column, ~1% is suggested to be in the surface ocean with the remaining 99% are simulated in the water column below the surface (Fig. 2). The model suggests a cascade of plastics from macro- to micro-, and eventually to uncatchable ones by fragmentation/abrasion, and 3.5% of the plastics in the surface ocean become uncatchable due to continuous fragmentation and abrasion. These masses make up the “missing” plastics from the surface ocean. Moreover, removal by the ingestion of marine organisms (Kühn et al., 2015), and interception by sea ice (Obbard et al., 2014), that are not included in our model, could also contain the “missing” plastics. But their importance may be much smaller than the beaching and sedimentation processes (Hardesty et al., 2017; van Sebille et al., 2020). The budget analysis also clearly indicates that the plastic in the seawater is not in a steady state, suggesting an increasing trend in concentrations.

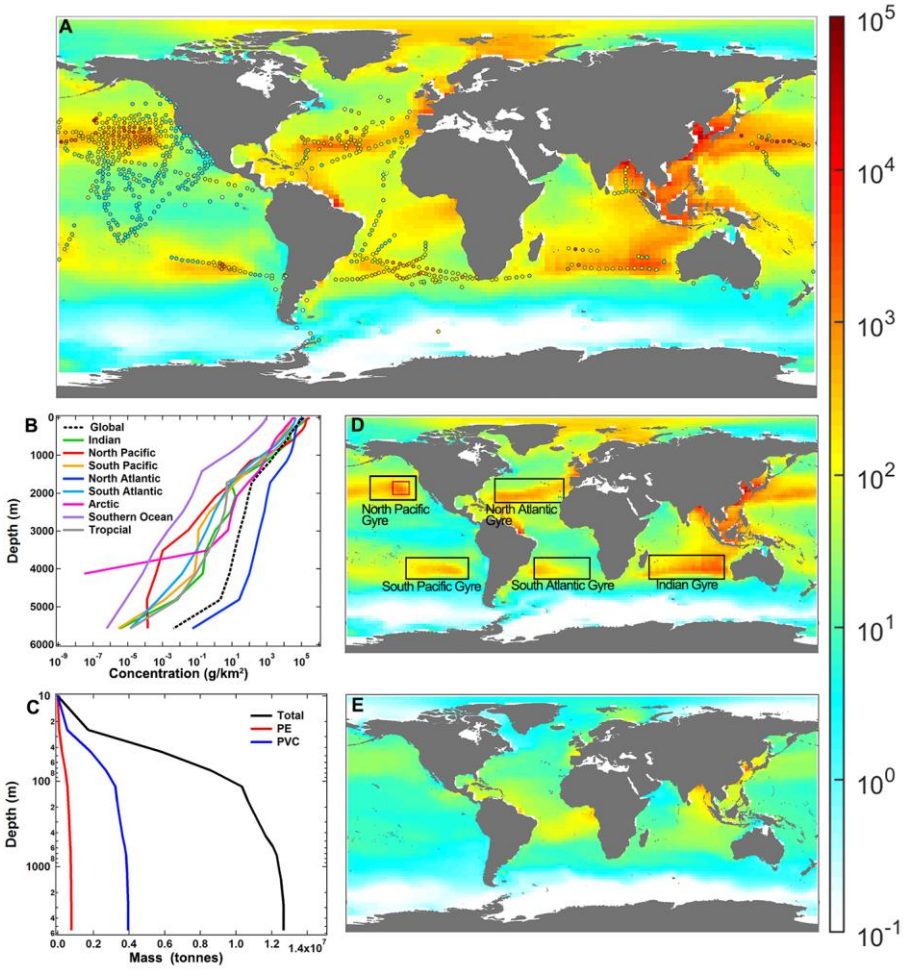

Fig. 1. Spatial pattern and vertical profiles of global marine plastics. (**A**) Modeled spatial pattern of catchable plastics (diameter > 0.33 mm) in the global ocean surface layer in 2010 [g km^{-2}]. Circles show observations between 2005 and 2015(Cozar et al., 2014 , Eriksen et al., 2014). (**B**) Vertical profiles of average plastic concentration in different ocean basins [g km^{-3}]. (**C**) Cumulative mass distribution of plastics in sediments with respect to the depth. (**D-E**), Modeled spatial distribution of PE (**D**) and PVC (**E**) in the global ocean surface layer in 2018 [g km^{-2}].

The model suggests that 92% of the plastics in seawater stay in the top 500 m (Fig. 2), as 60% of discharged plastics are light ones like PE and PP (Andrady, 2011). The modeled plastic concentrations decrease with depth in all ocean basins due to the dilution of a large volume of waters below the surface, however, there are also variabilities among basins (Fig. 1B). These profiles also have important implications for the large-scale transport of plastics by deep ocean currents given their long lifetime. This thus calls for sampling the subsurface waters as most of the current observations concentrate in the upper one-meter depth.

Relatively high fluxes of plastics buried by sediments are simulated near coasts (10^0-10^6 kg km^{-2}), where plastic waste is discharged, and denser plastics sink rapidly (Fig. 1C and Fig. S3B). Contrary to the hypothesis that deep seafloor is the major sink of plastics (Kane et al., 2020 , Woodall et al., 2014), the model simulates that seafloors shallower than 100 m receive 68% of the plastics in sediments (Fig. 1C). The biofouled low-density plastics (e.g. PE) are also most

frequently buried in the shallow seafloor near the coasts, where the abundance of nutrients favors the bloom of phytoplankton that facilitates biofouling (Ivan Valiela et al., 1997). Another important sink of plastics is the interception by sandy beaches (Fig. 2), which are distributed along the coasts (Fig. S3A). In all, the model indicates that 88% of the plastics are trapped in the upper ocean or coastal regions (Fig. 2), posing large ecological risk for pelagic and benthic ecosystems that are shallower than 500 m. However, the abundance of observational data over these regions so far has not been commensurate with this portion, and more data is needed to evaluate our projections.

The Arctic Ocean appears to be a dead-end for plastic debris due to the poleward transport from sub-polar North Atlantic Ocean (Fig. 1A). The Arctic Ocean seafloor (e.g. Barents Seas) is thus an important sink of marine plastics (Fig. S3B) (Cózar et al., 2017). The fluxes of plastics buried by seafloors are high in high-latitude North Atlantic Ocean and around Greenland and Barents Seas (10^3-10^6 g km^{-2}) (Fig. S3B), which is associated with deep water formation over this region (Cózar et al., 2017). Plastic sedimentation in this area accounts for 12% of the global total sedimentation fluxes. This is alarming to the vulnerable ecosystems in this region (Overland et al., 2014).

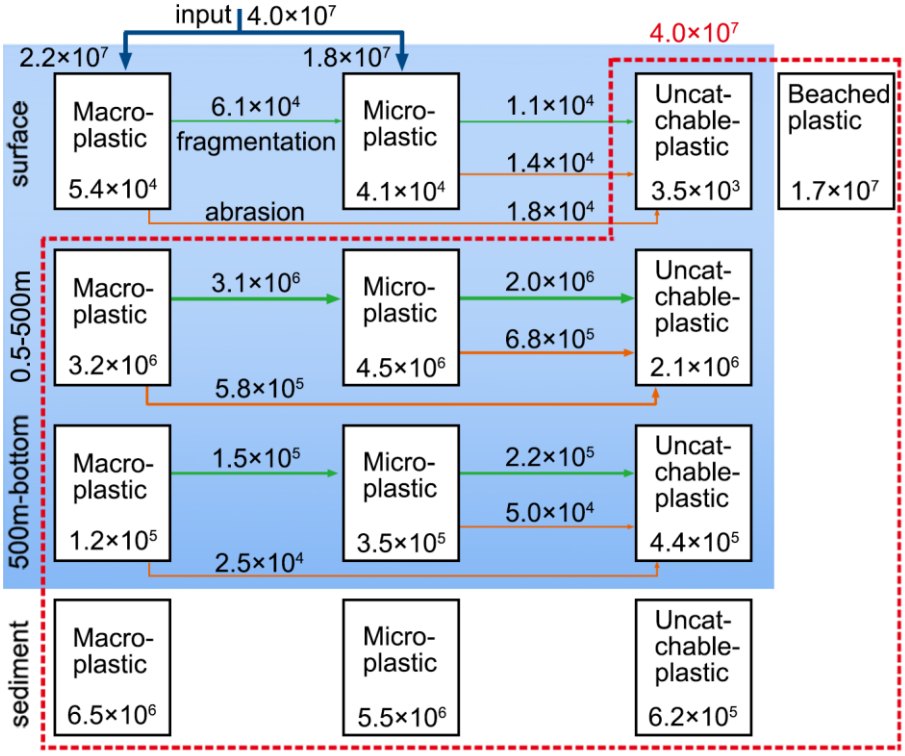

Fig. 2. Plastics mass budget for the global ocean from 1950 to 2018. The global ocean is divided into the surface (0 - 0.5 m), subsurface (0.5 - 500 m), 500 m-bottom, and sediment, respectively. The numbers below the tracer names are total mass. Red arrows indicate the input of mismanaged plastic waste; green arrows indicate the fragmentation; and orange arrows indicate the abrasion. All values are in the unit of tonnes. Missing plastics are framed by red dotted lines and the number in red on the top of the diagram is the total mass of missing plastics. Blue colors represent water columns.

Age of Plastics. By numerically tagging the discharges in different times and regions (see Methods), we find distinct spatial patterns for plastics with different ages and origins (Fig. 3). The plastics discharged before 1970 represent only 2.3% of the all-time releases and thus contribute little to today's marine plastics burden (Fig. 3A). Almost all of the oldest plastics are modeled to end up at the center of gyres (Fig. S4A-B), and the spatial pattern keeps almost unchanged in the last several decades of simulation. However, they are not the dominant contributor in these regions due to emission in 2000s and 2010s (elaborated in next section). Plastics discharged in the 1970s are modeled to dominate (about 34%) near Antarctica. It indicates that about 40 years are required for plastics to transport across the global oceans as ~90% of the plastics discharged in the 1970s were from the northern hemisphere. However, we need to emphasize that the modeled magnitudes of plastics in this remote region are extremely low due to continuously beaching, sinking, fragmentation, and abrasion (Fig. 1). The 40-year-old (i.e. discharged in the 1980s) plastics are still on their way to Antarctica and dominate in the high-latitude waters of the southern hemisphere. The plastics discharged in the 1990s and 2000s dominate in the lower latitudes than the 40-year-old ones. The youngest (10-year-old, discharged in 2010s) plastics are still relatively limited to the vicinity of their source regions with clear plumes extended downstream of major ocean currents (Fig. 3A, e.g. the Kuroshio in the North Pacific Ocean and the Gulf Stream in the tropical and North Atlantic Ocean).

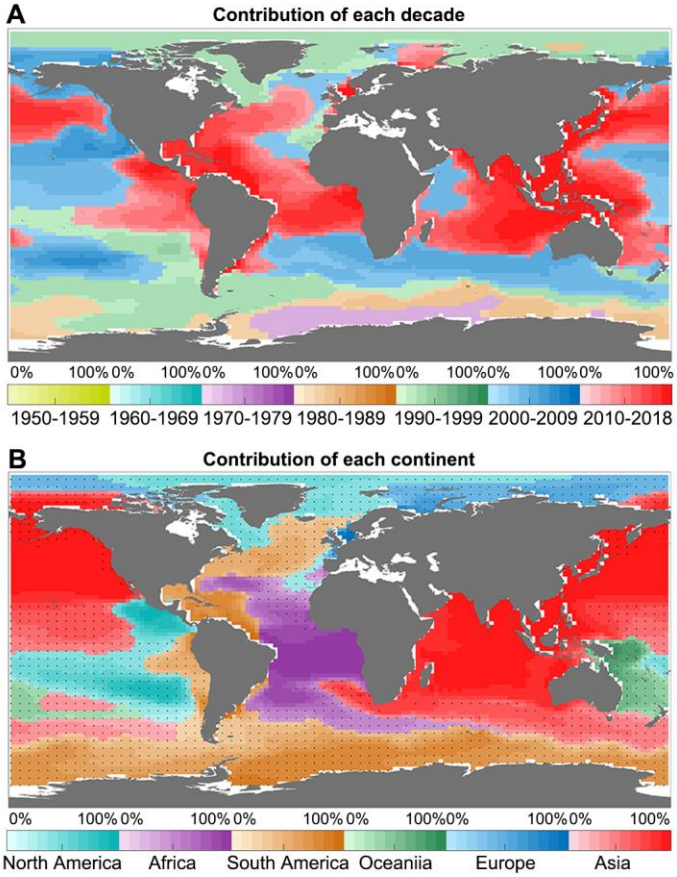

Fig. 3. The proportion of marine plastics in the surface ocean in 2018 from different sources. (**A**) Plastics in different ages. (**B**) Plastics from different continents. Color blocks in panel b indicate the contributions of each land sources without ocean sources, and the

superimposed dots indicate where the ocean source is dominant. The percentage contribution of each decade or continent (0-100%) increases as shade darkens.

The age of dominant plastics in the convergence zones in both hemispheres is relatively young compared to the length of the history of plastics (~70 years). The 10- and 20-year-old plastics account for 60% and 25% of the floating plastics there, respectively (Fig. 3A). This is consistent with the relatively young age found in the great pacific garbage patch by both recent studies (Lebreton et al., 2018) and earlier ones (Wong et al., 1974). Even though the 10-year old plastics begin to dominate in some of the 'garbage patches' (black boxes in Fig. 1C), the model suggests that only ~15% of the surface plastics discharged in the 2010s have reached the center of gyres and remote areas in the open ocean (Fig. S4G). It takes at least 10~20 years for most of the riverine discharged plastics to reach and accumulate to a significant level of concentrations in the convergence zones, longer than the travel time revealed by Lagrangian models (Lebreton et al., 2018 , Maximenko et al., 2012). As discharges during the 2010s account for 36% of all-time releases, which is much higher than the previous decades (Fig. S7), we thus expect a substantial further increase of plastic amount in these 'garbage patches' in the coming decades. It implies that improving solid waste management and curbing the discharge today will have immediate results in coastal regions, but may not take effect in these patches in 10-20 years.

The Origin of Plastics. The model indicates a widespread distribution of plastics dumped by shipping and fishing activities. This ocean dumping is the dominating source in 60% of ocean surface areas, although they only contribute 24% of surface plastic mass (Fig. 3B). They are the most widely distributed plastics and dominate in the Arctic, the Southern, the North Atlantic, and the South Pacific Ocean. The dumped plastics can reach areas far away from where shipping and fishing activities occur (Fig. S5A) because these plastics are directly discharged into the open ocean. Compared to the terrestrial sources which discharge at the shallow edge of the seas and oceans, debris in the open ocean is more easily transported and scattered. This calls for stricter observance to the international treaty MARPOL (International Convention for the Prevention of Pollution from Ships) that banned ships from dumping plastic waste into oceans.

The model allows us to directly relate the marine plastics to their region of release, which provides important source information to control the mass of floating plastics in different ocean basins. Excluding ocean dumping sources, Asian sources contribute 76% to the global plastic mass in the surface ocean, due to the large plastic discharge resulting from increasing population and rapid industrialization in recent decades. The most impacted regions by Asian sources are the North Pacific and Indian Ocean (Fig. 3B). North American sources are the largest contributor to the South Pacific (38% in mass) and Arctic Ocean (37% in mass) (Fig. S6), which is associated with its peak discharge in the 1980s and 1990s. Their contributions in the eastern North Pacific are smaller than that of Asian sources. Discharge from Europe gathers in the Arctic Ocean but its contribution to the Arctic Ocean (25% in mass) is smaller than North America. Sources from South America dominate 83% of the areas in the Southern Ocean due to its geographical proximity, but the absolute concentrations remain low (Fig. S5C). The African sources dominate in the South Atlantic Ocean (87% in mass) but their contributions in the Indian Ocean are surpassed by sources from Asia (Fig. S5B). Sources from Oceania gather in the surrounding western South Pacific Ocean and contribute 70% of the surface plastic mass there.

Uncertainty Analysis. Our study is subjected to uncertainty in the estimate of plastic emissions to the oceans (**Fig. 4 and Table S4**). The reported estimates of global riverine input of plastics vary by more than factors of two between the lower (Exp3 in Fig. 4) and upper (Exp2) bounds

(Lebreton et al., 2017). Other studies also suggest even higher mass of plastic entering the marine environment via rivers, fishing/shipping activities, and other pathways such as coastal erosion and groundwater discharge (Kershaw and Rochman, 2015). The historical discharge also has uncertainty as we assume the ratio of discharge to total use keeps constant (Geyer et al., 2017). Similarly, the model results are also sensitive to the emissions from marine activities and its temporal trends (especially after MARPOL).

The size distribution of the plastic input also matters. The Lebreton inventory does not consider the plastic larger than 2.5 cm and may underestimate the mass of total discharge (Van Emmerik et al., 2019 , Vriend et al., 2020). When using the plastic discharge fluxes estimated by Schmidt et al. (Schmidt et al., 2017) (Exp1), which assumes 94% of the global discharged as microplastics, the simulated macroplastics mass in the surface ocean account for less than 15% by present day (Table S4).

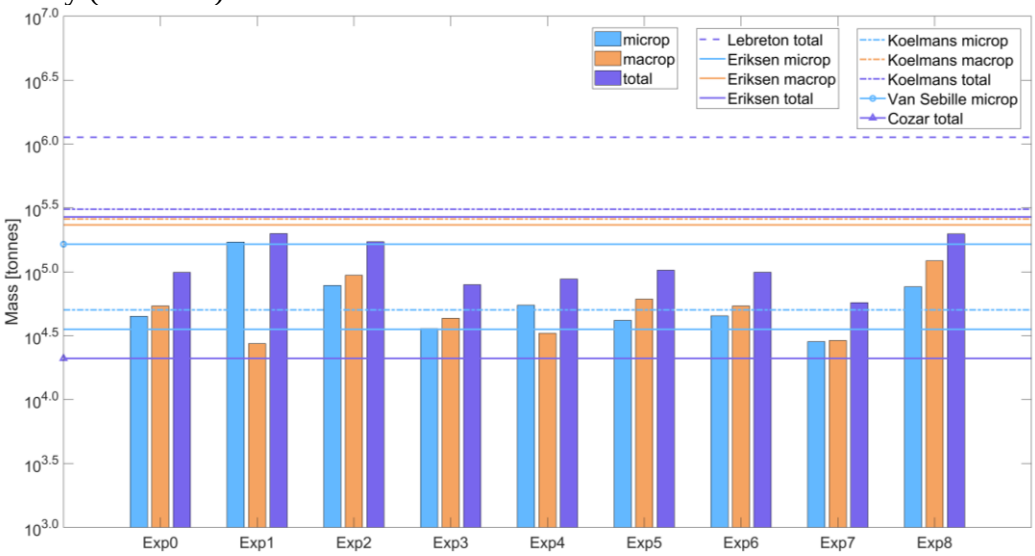

Fig. 4. The modeled mass of plastics in the surface ocean for different sensitivity simulations compared to previous studies (Lebreton et al., 2019 , Eriksen et al., 2014 , Koelmans et al., 2017 , Van Sebille et al., 2015 , Cozar et al., 2014). Exp0 (standard simulation): the riverine plastic discharge dataset is from midpoint estimate of Lebreton et al. (Lebreton et al., 2017), the degradation rate of all plastics is 1% $month^{-1}$, and the beaching rate is 10% day^{-1}. Exp1, the riverine plastic discharge dataset is from Schmidt et al. (Schmidt et al., 2017). Exp2: the riverine plastic discharge dataset is from upper estimate of Lebreton et al. (Lebreton et al., 2017). Exp3: the riverine plastic discharge dataset is from lower estimate of Lebreton et al. (Lebreton et al., 2017). Exp4: the fragmentation/abrasion rate of all plastics is 10% $month^{-1}$. Exp5: the fragmentation/abrasion rate of all plastics is 0.1% $month^{-1}$. Exp6: the fragmentation/abrasion rate of microplastics is 10% $month^{-1}$ and 1% $month^{-1}$ for macroplastics. Exp7: the beaching rate is 25% day^{-1}. Exp8: the beaching rate is 1% day^{-1}.

The spatial and temporal variability of marine plastic sources are also important factors. In the Lebreton inventory, only the large rivers within 60° North and South are considered, and Asian sources account for 67% of the global discharge. While in another study, the United States contributes the most in 2016 (Law et al., 2020). The riverine discharge fluxes estimated by Lebreton et al. (Lebreton et al., 2017) also unaccounted for deep layers, which could deliver high amounts of non-buoyant PVC and biofouled PE/PP to the seafloor (Morritt et al., 2013 ,

Pierdomenico et al., 2019). We find the uncertainty of emissions can be fully propagated to our estimate of plastic mass in the ocean (Fig. 4 and Table S4). Although we cover only selected possibilities in the uncertainty analysis, we expect an overall linear response for the environmental loads to further improved estimate of emissions.

Another source of uncertainty is the model representations of plastic transport and transformation processes. We choose the fragmentation/abrasion and beaching rates as an example to test the sensitivity of model results to these parameters, as a full evaluation of all schemes and parameters is computationally prohibitive. The fragmentation/abrasion rates are a function of environmental factors including light, temperature, oxygen and plankton biomass (Andrady, 2011). Even though perturbing this rate by a factor of 10 (Exp4 and 5) causes less than ~10% change for the total plastic mass in the surface ocean as the plastics are generally persistent in the ocean, the fraction of uncatchable plastics in surface plastics varies between 0.79% and 19% (Table S4). However, stronger fragmentation/abrasion generates more smaller-size particles. In another sensitivity simulation (Exp6), we specifically increase the fragmentation/abrasion rate of microplastics by 10 times (but keep that for macroplastics unchanged), as small plastics degrade faster than the large ones due to higher surface-area-to-volume ratio (Eriksen et al., 2014). The fraction of uncatchable plastics in the surface ocean also increases to 14%.

We find the beaching rate a major source of uncertainty, as beaches are a major reservoir for marine plastics (Lebreton et al., 2012) but the rate is largely unconstrained. The rates of both beaching and resuspension and the eventual residence time of plastics on beaches depend on the characteristics of plastics, the coastal morphological features, wind, and wave conditions (Zhang, 2017 , Kaandorp et al., 2020 , Hinata et al., 2017 , Lebreton et al., 2019). Our calculated overall beaching ratio (42%) is consistent with a previous study for the Mediterranean (49-63%) (Kaandorp et al., 2020). Perturbating the beaching rate from 1% to 25% day^{-1} (Exp8 and 7, respectively) results that the beached plastics account for 8-62% of total discharge (Table S4). The simulated total mass in the surface ocean also varies form 5.7×10^4 to 2.0×10^5 tonnes, indicating a high sensitivity.

These uncertainty ranges reflect our current understanding of these processes (Hardesty et al., 2017 , Van Sebille et al., 2020). The general agreement between the model results and the observations over the surface ocean may result from the cancellation of different uncertainties. Our assessment is thus designed to be illustrative, calling for further studies to improve the riverine discharge estimate and the rates of important plastic processes (e.g. fragmentation/abrasion and beaching) (Hardesty et al., 2017). Therefore, the model result should not be taken as a comprehensive simulation of the fate of plastics. However, the relative temporal and spatial patterns and trends are more robust than the absolute amounts. As scientific knowledge evolves, our mechanical model framework could be improved using similar methodology. One drawback of this study is not considering the bi-directional exchange between beaches and the coastal waters as well as the resuspension of sunk plastics in the sediments. This also indicates the necessity of an Earth System modeling approach to incorporate the sediment, beaches, water columns, and the ecosystems therein.

Policy Implications. Ocean plastics' research has focused on convergence zones that tend to be oligotrophic regions with relatively low productivity (Westberry et al., 2008). Our work reveals more complex spatial patterns for the distributions of plastics with different ages and source origins. We identify potentially new garbage patches in regions that are also important habitats

for commercial catch fishes (Watson, 2017), such as the coastal and downstream regions of Asia and Western Europe. The increasing plastic waste reaching the oceans poses a growing threat to the survival of marine organisms (Jambeck et al., 2015). In addition, plastics that remain in the seawater become increasingly threatening, as they have been detected to be able to break into nanoplastics (Halle et al., 2017), whose trophic transfer and ecological toxicity have been described in experimental studies (Tommy Cedervall et al., 2012). More measurements in these regions are in urge need to confirm our projections.

The ubiquity of marine plastics and their long-range transport potential revealed by this study indicate the necessity of global controlling efforts, such as the market-based instruments, policies, regulations, and legislation to reduce marine debris, as proposed by the Honolulu Strategy (UNEP 2012). Based on the spatial pattern of plastics in the global ocean, the North Pacific and the Indian Ocean are the "hard-hit" regions that are most impacted by Asian sources. The newly discharged plastic waste remains close to coastlines. And most have not yet broken down to smaller sizes, which can be easier to remove from the sea by ordinary capture methods. In the coming years, efforts to control plastic discharge in these countries, such as banning single-use plastic products, improving the waste collection system and infrastructure, and controlling illegal dumping and landfills are essential steps to mitigate the global plastic problem.

Methods

General description of the model. We simulate the fate and transport of plastics in the MITgcm model framework (Marshall et al. 1997). This model is Euler-based and simulates the emission, transport, diffusion, sinking, and transformation (including biofouling, fragmentation, and abrasion) of plastics in each model grid cell. The model has a resolution of 2°×2.5° horizontally with 22 vertical levels, and a time step is of 4 hours. The ocean circulation data is from the Integrated Global Systems Model (IGSM) (Dutkiewicz et al. 2005). The ocean boundary layer physics is modeled based on Large et al. (1994), and the effects of mesoscale eddies on isopycnal mixing are parameterized following Gent and McWilliams (1990). We run the model from 1950 to 2018. The model has a relatively coarse resolution to resolve the currents over coastal regions and western boundary currents such as Kuroshio and Gulf Stream but perform better over the open ocean (Dutkiewicz et al. 2005). The lower computational costs compared to high-resolution models also allow us to perform long-term and multiple-scenario runs. We test different time steps and the results keep relatively robust due to the low stiffness in simulating these processes. The model includes a total of 54 plastic tracers. Plastics are divided into four categories according to the chemical composition and the density of each category is pre-determined: PE (950 kg m^{-3}), PP (900 kg m^{-3}), PVC (1410 kg m^{-3}), and others (1050 kg m^{-3}). The plastic's density is increased when biofouled. Each category has six size bins: four for microplastics: <0.0781 mm, 0.0781-0.3125 mm, 0.3125-1.25 mm, and 1.25-5 mm, and two for macroplastics: 5-50 mm and >50 mm.

We develop a universal framework for the transport of these tracers in the global ocean. Tracking the three-dimensional motion of microplastics is distinct from estimating other trace components in ocean models. Since plastics particles have non-negligible volume and different density with the seawater. Obtaining closed expressions describing the hydrodynamic forces experienced by rigid particles embedded in various flows has been a subject of active research for a long time (Magnaudet 1997). Equations could be selected and simplified, based on facts, to help the simulation. Most of the time in the global ocean, light particles (PP and PE) float and

drift in quasi-two-dimensional motion relative to the sea surface. Besides, light particles would sink after becoming heavier than seawater by biofouling, and rise after defouling. These particles would also rise, once got immersed in water by convection and turbulence. Other particles that have a higher density than the seawater (e.g. PVC), would instantly sink after dumped. Sinking or rising particles make an approximate one-dimensional motion relative to the water column. Thus, in our model, the motion of plastic particles is resolved into seawater transportation (three-dimensional), sinking/rising (one-dimensional), and drifting (two-dimensional). We calculate particles' sinking, rising, and drifting velocity by dynamics and experiential equations. Without loss of generality, plastics particles in our model are treated as smooth rigid spheres. These processes are elaborated on in the sections below.

Plastic sources. We use the riverine plastic discharge dataset from Lebreton et al. considering the seasonality, spatial variability, and size distribution of local sources (Lebreton et al. 2017). This dataset estimates plastic discharge based on waste management, population density, and hydrological information. The total discharge is divided into micro- and macroplastics according to the ratio of micro and macroplastics in sampled rivers. We also consider direct ocean emissions from marine activities such as shipping and fishing, which is 25% of riverine discharge (Faris and Hart 1994; Macfadyen, Huntington, and Cappell 2009). The discharge from marine activities is allocated spatially according to the global footprint of fisheries (Kroodsma et al. 2018). The historical trend of plastic discharge during 1950-2018 is from Isobe et al. (Isobe et al. 2019) and Plastics Europe (https://www.plasticseurope.org/en/resources/market-data). The historical trend of plastic discharge from each continent is assumed to follow that of per-capita GDP (https://data.worldbank.org/). The discharge of each type of plastics is calculated based on its proportion in global consumption (China Plastic 2014).

Sinking and rising. The sinking or rising speed of plastic particles depends on its density, diameter, shape, and the seawater state. In a steady state, plastic particles have the same horizontal velocity as the seawater around, and three balanced vertical forces acting on the particles:

$$\mathbf{F_g} = V_p \rho_p \mathbf{g} \tag{1}$$

$$\mathbf{F_b} = -V_s \rho_s \mathbf{g} \tag{2}$$

$$\mathbf{F_D} = -\frac{1}{2} \mathrm{C_D}(Re_s) A_p \rho_s \frac{(\mathbf{u}-\mathbf{u_s})^3}{|\mathbf{u}-\mathbf{u_s}|} \tag{3}$$

$$\mathbf{F_D} + \mathbf{F_g} + \mathbf{F_b} = 0 \tag{4}$$

where F_D is vertical dragging force, F_g is gravity, and F_b is buoyancy. V_p is the volume of the particle, while V_s is the volume of particle that is submerged in seawater (in this case, $V_p = V_s$). C_D is the coefficient of dragging, which is a function of the Reynolds number (Re) of a certain motion of a fluid. A_p is the horizontal sectional area of a particle, ρ_s is the density of seawater, d is Stokes diameter of a particle, ρ_p is the mean density of a particle, **u** is the velocity of the particle relative to the seawater, and **g** is the gravity acceleration.

Based on Equation (1)-(4), we get:

$$\mathbf{u}^2 = \frac{4|\mathbf{g}|d(\rho_p - \rho_s)}{3\mathrm{C_D}(Re_s)\rho_s} \tag{5}$$

while C_D is calculated as:

$$\mathrm{C_D}(Re) = \begin{cases} 24Re^{-1} & Re \le 0.3 \\ 18.5Re^{0.6} & 0.3 < Re \le 1000 \\ 0.44 & 1000 < Re \le 20000 \end{cases} \tag{6}$$

Re_s is the Re of seawater and is calculated as:

$$Re_s = \frac{d\rho_s|\mathbf{u} - \mathbf{u_s}|}{\mu_s} \tag{7}$$

where μ_s is the dynamic viscosity of seawater. By substituting Eq. (6) and (7) into Eq. (5), with few techniques, we can solve **u** (Flemmer and Banks, 1986). In this way, we get the rising or sinking speed of the particles, by which we simulate the vertical transport of the plastics particles in the seawater columns (More details see Table S2).

Drifting. Plastic particles floating on the sea surface are subject to wind forces, which are commonly referred to as leeway drift, or windage (Hackett, Breivik, and Wettre 2006). The motion of a drifting particle in balance, which is affected by five forces (gravity, buoyancy, seawater stress, horizontal wind stress, and Coriolis force), is described by equations (1), (2), (8), (9), (10), respectively.

$$\mathbf{F_s} = -\frac{1}{2}\mathrm{C_D}(\mathrm{Re}_s)A_s\rho_s\frac{(\mathbf{u} - \mathbf{u_s})^3}{|\mathbf{u} - \mathbf{u_s}|} \tag{8}$$

$$\mathbf{F_a} = -\frac{1}{2}\mathrm{C_D}(\mathrm{Re}_a)A_a\rho_a\frac{(\mathbf{u} - \mathbf{u_a})^3}{|\mathbf{u} - \mathbf{u_a}|} \tag{9}$$

$$\mathbf{F_c} = V_p\rho_p f\mathbf{u} \tag{10}$$

$$Re_a = \frac{d\rho_a|\mathbf{u} - \mathbf{u_a}|}{\mu_a} \tag{11}$$

where subscript p is for particle, a is for air (or wind), and s is for seawater. **u**, $\mathbf{u_s}$ and $\mathbf{u_a}$ are the velocity of plastic particles, seawater, and wind, respectively. A_a and A_s are the vertical sectional areas of particles exposed to the air and seawater, respectively. ρ_a and Re_a are the density and the Reynolds number of air, respectively. μ_a is the dynamic viscosity of air. *f* is the Coriolis parameter.

We assume the vertical forces act on the particle reach a balance:

$$\mathbf{F_g} + \mathbf{F_b} = 0 \tag{12}$$

with which we can solve the V_s (in this case, $V_s < V_p$) and subsequently A_a and A_s based on geometry. $C_D(Re_a)$ and $C_D(Re_s)$ are calculated as functions of Reynolds number of air (Eq. 11) and seawater (Eq. 7), respectively, based on Eq. 6.

We solve **u** by assuming the horizontal forces $\mathbf{F_a}$ and $\mathbf{F_s}$ reach a balance while $\mathbf{F_c}$ is neglected due to a much smaller magnitude:

$$\mathbf{F_a} + \mathbf{F_s} = 0 \tag{13}$$

By substituting eq. (8) and eq. (9) into eq. (13), we solve **u** numerically by a gradient descent method (Table S3). This leads to a constant drifting speed **u** given $\mathbf{u_a}$ and $\mathbf{u_s}$. The $\mathbf{u_a}$ is from NCEP/NCAR reanalysis (Kalnay et al., 1996). The random walk of plastic particles caused by oceanic eddy turbulence with a horizontal scale that is smaller than the grid size is simulated as an isopycnal diffusion process in the model. The stokes drift process of plastic particles is also not included due to the lack of ocean wave conditions in the model. In our model, drifting velocity is treated as a correction of ocean tracer.

Fragmentation/Abrasion. Fragmentation represents the process during which large plastics break up into smaller ones. Abrasion refers to the process in which tiny plastics peel off from the surface of larger ones, usually caused by mechanical shearing (White and Turnbull 1994). In the model, we assume 0.9% of plastic in each size bin breaks into particles one size bin smaller per month, while an additional 0.1% is transferred to the smallest size bin (Niaounakis 2017). In the surface ocean, we consider an additional photo-degradation process if the plastic particles are not biofouled. The rate (R) is proportional to the downward shortwave radiation q:

$$R[\%] = \begin{cases} (\frac{0.005}{175}) \cdot q + 0.005 & q \le 175\mathrm{W} \cdot \mathrm{m}^{-2} \\ (\frac{0.001}{175}) \cdot q & q > 175\mathrm{W} \cdot \mathrm{m}^{-2} \end{cases} \tag{14}$$

The surface downward shortwave radiation is taken from the CMIP5 project.

Beaching. A plastic particle is 'beached' when it arrives at a beach-adjacent cell. The beaching rate is geographically diverse depending on the coastal morphological features, wind, and wave conditions. Previous studies suggest that beached plastics can be eroded back to the ocean, and bi-directional exchanges occur between the beach and coastal seawaters (Lebreton, Egger, and Slat 2019). Atwood et al. found <10-94% of released plastics are beached and the majority of beaching occurs within the first 3 days (Atwood et al. 2019). Ocean drifter studies reveal that the timescales of the beaching and resuspension processes range from several weeks to months under different conditions (Samaras et al. 2014; Hinata et al. 2017; Stanev et al. 2019). We consider a net beaching rate (i.e. beaching - resuspension) in this study due to the large uncertainty of the two processes. We assume that the plastics in grid cells immediately adjacent to sandy beaches are partially removed from the seawater and the mass of beached plastics is proportional to the length of the beach in the cell. We assume a conservative beaching rate of 10% per day. The global sandy beaches dataset is from Luijendijk et al. (Luijendijk et al. 2018).

Biofouling and defouling. Biofouling of light plastic types (PE and PP) is modeled following Kooi et al. (Kooi et al. 2017) but adjusted for more realistic scenarios. Three stages with different degrees of biological attachment are considered: clean, balanced, and sinking. Clean plastics have no biomass attached and stay floating on the sea surface with the same density as the original plastic materials. Balanced plastics are the same density as seawater and suspend in water columns. Sinking plastics are heavier than seawater and sink to the subsurface ocean. The biomass of phytoplankton in global oceans is used as a proxy to scale the overall biofouling

potential from phytoplankton, zooplankton, marine snow, and the ingestion and inclusion in feces. The phytoplankton biomass data is taken from the MITgcm Darwin ecosystem model (Follows et al. 2007). Using phytoplankton as a proxy might introduce uncertainty as the community structure varies drastically in different ocean biogeoprovinces. The Darwin model also does not consider the vertical migrations of zooplankton. But it is relatively robust as it is constrained by satellite remote sensing data (Dutkiewicz, Follows, and Bragg 2009). Especially, the phytoplankton distribution suggests stronger biofouling in productive coastal waters than the open ocean, consistent with empirical studies (Cole et al. 2011).

The volume of biomass on plastic particles (V_{bf}) depends on the algae volume V_a, the number density of attached algae per unit area A (# m^{-2}) and the surface area of the plastic particle θ_p:

$$\frac{dV_{bf}}{dt} = V_a \theta_p \frac{dA}{dt} + V_a A \frac{d\theta_p}{dt} \tag{15}$$

where:

$$\frac{dA}{dt} = \frac{\beta_a A_a}{\theta_p} - m_a A \tag{16}$$

where β_a is the encounter kernel rate (m^3 s^{-1}), A_a is the ambient algae concentration (# m^{-3}), and m_a is the mortality rate (s^{-1}). The encounter kernel rate β_a is the sum of Brownian motion and advective shear collision frequencies (m^3 s^{-1}):

$$\beta_a = \beta_{brownian} + \beta_{shear} \tag{17}$$

where:

$$\beta_{brownian} = 4\pi(D_p + D_a)(r_p + r_a) \tag{18}$$

$$\beta_{shear} = 1.3\gamma(r_p + r_a)^3 \tag{19}$$

$$D_p = \frac{k(T + 273.16)}{6\pi\mu_{sw} r_p} \tag{20}$$

$$D_a = \frac{k(T + 273.16)}{6\pi\mu_{sw} r_a} \tag{21}$$

where D_p and D_a are the diffusivity of plastics and the individual algae cells (m^2 s^{-1}), respectively, r_p and r_a are the radius of plastics and the individual algae cells, respectively, γ is the shear rate (s^{-1}), κ is the Boltzmann constant (m^2 kg s^{-2} K^{-1}), T is the temperature (°C), and μ_{sw} is the dynamic water viscosity (kg m^{-1} s^{-1}) (More details see Table S4).

The transformation rate between different types of plastics τ_{trans} (s^{-1}) is calculated as:

$$\tau_{trans} = \delta \frac{\frac{dV_{bf}}{dt}}{\Delta V} \tag{22}$$

where δ is an adjustable coefficient tuned to match the result of Kooi et al. (2017), and ΔV is the deviation between the volumes of two plastic types, e.g.:

$$\Delta V(PE_{balanced}, PE_{clean}) = V_{PE_{balanced}} - V_{PE_{clean}} \quad (23)$$

Data availability

All data are available in the group web site: https://www.ebmg.online/model_plastics.html.

Code availability

All model code is available at the research group website: https://www.ebmg.online/model_plastics.html.

References

Andrady A L 2011. Microplastics in the marine environment. Marine Pollution Bulletin [J], 62: 1596-1605.

Atwood E C, FALCIERI F M, PIEHL S, et al. 2019. Coastal accumulation of microplastic particles emitted from the Po River, Northern Italy: Comparing remote sensing and hydrodynamic modelling with in situ sample collections. Marine Pollution Bulletin [J], 138: 561-574.

China Plastic. China plastics industry yearbook 2014[C]//,2014

Cole M, Lindeque P, Halsband C, et al. 2011. Microplastics as contaminants in the marine environment: a review. Marine Pollution Bulletin [J], 62: 2588-2597.

Cozar A, F Echevarria, J Ignacio Gonzalezgordillo, et al. 2014. Plastic debris in the open ocean. Proceedings of the National Academy of Sciences of the United States of America [J], 111: 10239-10244.

Cózar A, Martí E, Duarte C M, et al. 2017. The Arctic Ocean as a dead end for floating plastics in the North Atlantic branch of the Thermohaline Circulation. Science Advances [J], 3: e1600582.

Dutkiewicz S, Follows M J, Bragg J G 2009. Modeling the coupling of ocean ecology and biogeochemistry. Global Biogeochemical Cycles [J], 23.

Dutkiewicz S, Sokolov A P, Scott J, et al. 2005. A Three-Dimensional Ocean-Seaice-Carbon Cycle Model and its Coupling to a Two-Dimensional Atmospheric Model: Uses in Climate Change Studies. Mit Joint Program on the Science & Policy of Global Change [J].

Eriksen M, Lebreton L C, Carson H S, et al. 2014. Plastic pollution in the world's oceans: More than 5 trillion plastic pieces weighing over 250,000 tons afloat at sea. PLOS ONE [J], 9: e111913.

Faris J, Hart K 1994. Sears of debris: A summary of the third International Conference on Marine Debris. N.C. Sea Grant College Program and NOAA. [J].

Flemmer R.L.C., Banks C.L. 1986. On the drag coefficient of a sphere, Powder Technology [J]

Fischer V, Elsner N O, Brenke N, et al. 2015. Plastic pollution of the Kuril–Kamchatka Trench area (NW pacific). Deep-sea Research Part Ii-topical Studies in Oceanography [J], 111: 399-405.

Follows M J, Dutkiewicz S, Grant S, et al. 2007. Emergent Biogeography of Microbial Communities in a Model Ocean. Science [J], 315: 1843-1846.

Gent P R, Mcwilliams J C 1990. Isopycnal mixing in ocean circulation models. Journal of Physical Oceanography [J], 20: 150-155.

Geyer R, Jambeck J R, Law K L 2017. Production, use, and fate of all plastics ever made. Science Advances [J], 3: e1700782.

Gregory M R 2009. Environmental implications of plastic debris in marine settings—entanglement, ingestion, smothering, hangers-on, hitch-hiking and alien invasions. Philosophical Transactions of the Royal Society B: Biological Sciences [J], 364: 2013-2025.

Hackett B, Breivik Ø, Wettre C. Forecasting the drift of objects and substances in the ocean[C]//Ocean weather forecasting.Springer,2006:507-523.

Halle A T, Orcid L J, Martignac M, et al. 2017. Nanoplastic in the North Atlantic subtropical gyre. Environmental Science & Technology [J], 51: 13689–13697.

Hardesty B D, Harari J, Isobe A, et al. 2017. Using numerical model simulations to improve the understanding of micro-plastic distribution and pathways in the marine environment. Frontiers in Marine Science [J], 4: 30.

Hinata H, Mori K, Ohno K, et al. 2017. An estimation of the average residence times and onshore offshore diffusivities of beached microplastics based on the population decay of tagged meso-and macrolitter. Marine Pollution Bulletin [J], 122: 17-26.

Isobe A, Iwasaki S, Uchida K, et al. 2019. Abundance of non-conservative microplastics in the upper ocean from 1957 to 2066. Nature Communications [J], 10: 417.

Ivan Valiela, James W Mcclelland, Jennifer Hauxwell, et al. 1997. Macroalgal blooms in shallow estuaries: Controls and ecophysiological and ecosystem consequences. Limnology and Oceanography [J], 42: 1105-1118.

Jambeck J R, Geyer R, Wilcox C, et al. 2015. Plastic waste inputs from land into the ocean. Science [J], 347: 768-771.

Kalnay et al.,The NCEP/NCAR 40-year reanalysis project, Bull. Amer. Meteor. Soc., 77, 437-470, 1996.

Kaandorp M L A, Dijkstra H A, Van Sebille E 2020. Closing the Mediterranean marine floating plastic mass budget: inverse modeling of sources and sinks. Environmental Science & Technology [J], 54: 11980–11989.

Kane I A, Clare M A, Miramontes E, et al. 2020. Seafloor microplastic hotspots controlled by deep-sea circulation. Science [J]: eaba5899.

Kershaw P J, Rochman C M 2015. Sources, fate and effects of microplastics in the marine environment: part 2 of a global assessmen. Reports and Studies-IMO/FAO/Unesco-IOC/WMO/IAEA/UN/UNEP Joint Group of Experts on the Scientific Aspects of Marine Environmental Protection (GESAMP) Eng No. 93 [J].

Koelmans A A, Kooi M, Law K L, et al. 2017. All is not lost: deriving a top-down mass budget of plastic at sea. Environmental Research Letters [J], 12: 114028.

Kooi M, Van Nes E H, Scheffer M, et al. 2017. Ups and downs in the ocean: Effects of biofouling on the vertical transport of microplastics. Environmental Science & Technology [J], 51: acs.est.6b04702.

Kroodsma D A, Juan Mayorga, Timothy Hochberg, et al. 2018. Tracking the global footprint of fisheries. Science [J], 359: 904-908.

Kühn S, Rebolledo E L B, Van Franeker J A. Deleterious effects of litter on marine life[C]//Marine anthropogenic litter.Springer, Cham,2015:75-116.

Lacerda A L D F, Rodrigues L D S, Van Sebille E, et al. 2019. Plastics in sea surface waters around the Antarctic Peninsula. Scientific Reports [J], 9: 3977.

Large W G, Mcwilliams J C, Doney S C 1994. Oceanic vertical mixing: A review and a model with a nonlocal boundary layer parameterization. Reviews of Geophysics [J], 32: 363-403.

Law K L, Starr N, Siegler T R, et al. 2020. The United States' contribution of plastic waste to land and ocean. Science Advances [J], 6: eabd0288.

Lebreton L, Egger M, Slat B 2019. A global mass budget for positively buoyant macroplastic debris in the ocean. Scientific Reports [J], 9: 12922.

Lebreton L, Greer S, Borrero J C 2012. Numerical modelling of floating debris in the world's oceans. Marine Pollution Bulletin [J], 64: 653-661.

Lebreton L, Slat B, Ferrari F, et al. 2018. Evidence that the Great Pacific Garbage Patch is rapidly accumulating plastic. Scientific Reports [J], 8: 4666.

Lebreton L C M, Van Der Zwet J, Damsteeg J-W, et al. 2017. River plastic emissions to the world's oceans. Nature Communications [J], 8: 15611.

Luijendijk A, Hagenaars G, Ranasinghe R, et al. 2018. The state of the world's beaches. Scientific Reports [J], 8: 6641-6641.

Lusher A L, Tirelli V, O'Connor I, et al. 2015a. Microplastics in Arctic polar waters: the first reported values of particles in surface and sub-surface samples. Scientific Reports [J], 5: 14947.

Lusher A L, Tirelli V, O'Connor I, et al. 2015b. Microplastics in Arctic polar waters: the first reported values of particles in surface and sub-surface samples. Scientific Reports [J], 5: 14947.

Macfadyen G, Huntington T, Cappell R 2009. Abandoned, lost or otherwise discarded fishing gear. UNEP Regional Seas Reports and Studies No.185; FAO Fisheries and Aquaculture Technical Paper, No. 523.UNEP/FAO [J].

Marshall J, Adcroft A, Hill C, et al. 1997. A finite-volume, incompressible Navier-Stokes model for studies of the ocean on parallel computers. J Geophys Res 102(C3):5753-5766. Journal of Geophysical Research Oceans [J], 102: 5753-5766.

Mato Y, Isobe T, Hideshige Takada, et al. 2001. Plastic resin pellets as a yransport medium for toxic chemicals in the marine environment. Environmental Science & Technology [J], 35: 318-324.

Maximenko N, Hafner J, Niiler P 2012. Pathways of marine debris derived from trajectories of Lagrangian drifters. Marine Pollution Bulletin [J], 65: 51-62.

Morritt D, Stefanoudis P V, Pearce D, et al. 2013. Plastic in the Thames: A river runs through it. Marine Pollution Bulletin [J], 78: 196-200.

Mountford A S, Morales Maqueda M A 2019. Eulerian modeling of the three‐dimensional distribution of seven popular microplastic types in the global ocean. Journal of Geophysical Research: Oceans [J], 124: 8558–8573.

Niaounakis M. Degradation of plastics in the marine environment[C]//Management of Marine Plastic Debris.2017:127-142.

Obbard R W, Sadri S, Wong Y Q, et al. 2014. Global warming releases microplastic legacy frozen in Arctic Sea ice. Earth's Future [J], 2: 315-320.

Overland J E, Wang M, Walsh J E, et al. 2014. Future Arctic climate changes: Adaptation and mitigation time scales. Earth's Future [J], 2: 68-74.

Peeken I, Primpke S, Beyer B, et al. 2018. Arctic sea ice is an important temporal sink and means of transport for microplastic. Nature Communications [J], 9: 1505.

Pierdomenico M, Casalbore D, Chiocci F L 2019. Massive benthic litter funnelled to deep sea by flash-flood generated hyperpycnal flows. Scientific Reports [J], 9: 1-10.

Reisser J, Shaw J, Wilcox C, et al. 2013. Marine Plastic Pollution in Waters around Australia: Characteristics, Concentrations, and Pathways.

Samaras A G, Dominicis M D, Archetti R, et al. 2014. Towards improving the representation of beaching in oil spill models: A case study. Marine Pollution Bulletin [J], 88: 91-101.

Schmidt C, Krauth T, Wagner S 2017. Export of plastic debris by rivers into the sea. Environmental Science & Technology [J], 51: 12246-12253.

Stanev E V, Badewien T H, Freund H, et al. 2019. Extreme westward surface drift in the North Sea: public reports of stranded drifters and Lagrangian tracking. Continental Shelf Research [J], 177.

Teuten E L, Saquing J M, Knappe D R U, et al. 2009. Transport and release of chemicals from plastics to the environment and to wildlife. Philosophical Transactions of the Royal Society B: Biological Sciences [J], 364: 2027-2045.

Tommy Cedervall, Larsanders Hansson, Mercy Lard, et al. 2012. Food chain transport of nanoparticles affects behaviour and fat metabolism in fish. PLOS ONE [J], 7.

Van Emmerik T, Loozen M, Oeveren K V, et al. 2019. Riverine plastic emission from Jakarta into the ocean. Environmental Research Letters [J], 14.

Van Sebille E, Aliani S, Law K L, et al. 2020. The physical oceanography of the transport of floating marine debris. Environmental Research Letters [J], 15.

Van Sebille E, England M H, Froyland G 2012. Origin, dynamics and evolution of ocean garbage patches from observed surface drifters. Environmental Research Letters [J], 7.

Van Sebille E, Wilcox C, Lebreton L, et al. 2015. A global inventory of small floating plastic debris. Environmental Research Letters [J], 10: 124006.

Vriend P, Roebroek C T J, Van Emmerik T 2020. Same but different: A framework to design and compare riverbank plastic monitoring strategies. Frontiers in Water [J], 2.

Watson R 2017. A database of global marine commercial, small-scale, illegal and unreported fisheries catch 1950–2014. Scientific Data [J], 4: 1-9.

Westberry T K, Behrenfeld M J, Siegel D, et al. 2008. Carbon-based primary productivity modeling with vertically resolved photoacclimation. Global Biogeochemical Cycles [J], 22.

White J R, Turnbull A 1994. Weathering of polymers: mechanisms of degradation and stabilization, testing strategies and modelling. Journal of Materials Science [J], 29: 584-613.

Wichmann D, Delandmeter P, Van Sebille E 2019. Influence of near‐surface currents on the global dispersal of marine microplastic. Journal of Geophysical Research [J], 124.

Wong C S, Green D R, Cretney W J 1974. Quantitative tar and plastic waste distributions in the Pacific Ocean. Nature [J], 247: 30-32.

Woodall L C, Sanchez-Vidal A, Canals M, et al. 2014. The deep sea is a major sink for microplastic debris. Royal Society Open Science [J], 1: 140317.

Zhang H 2017. Transport of microplastics in coastal seas. Estuarine, Coastal and Shelf Science [J], 199: 74-86.

Acknowledgments

This research was funded by National Natural Science Foundation of China (NNSFC) 41875148, Jiangsu Innovative and Entrepreneurial Talents Plan, the Collaborative Innovation Center of Climate Change, Jiangsu Province. The authors thank Theodore Vincent for reading through the manuscript.

Author contributions

Y.Z. conceived and designed the research. P.W., X.W. and R.X. performed the data analyses and produced the figures. A.L. obtained the beach dataset. P.W., R.X., X.W., Y.Z., and A.S. wrote the paper. All authors contributed to the scientific discussions and preparation of the manuscript.

Competing interests

Authors declare no competing interests.

Additional information

Additional data and figures are provided in the Supplementary information.